



Experimental and theoretical analysis of molecular structure, vibrational spectra and biological properties of the new Co(II), Ni(II) and Cu(II) Schiff base metal complexes

R.V. Sakthivel^a, P. Sankudevan^a, P. Vennila^{b,*}, G. Venkatesh^c, S. Kaya^d, G. Serdaroglu^e

^a Department of Chemistry, Aringar Anna Government Arts College, Namakkal-637 002, India

^b Department of Chemistry, Thiruvalluvar Government arts college, Rasipuram-637 401, India

^c Department of Chemistry, VSA Group of Institutions, Salem- 636010, India

^d Department of Chemistry, Cumhuriyet University, Sivas-58140, Turkey

^e Sivas Cumhuriyet University, Faculty of Education, Math. and Sci. Edu. 58140, Sivas, Turkey

ARTICLE INFO

Article history:

Received 21 November 2020

Revised 5 February 2021

Accepted 5 February 2021

Available online 15 February 2021

Keywords:

Schiff base

Ultraviolet-visible

Geometrical parameters

Antioxidant activity

Molecular docking

ABSTRACT

A new novel Cobalt, Nickel and Copper metal complexes were synthesized from Schiff base ligand of 2,2'-(1E,1'E)-((4-nitro-1,2-phenylene) bis(azanylylidene)) bis(methanylylidene)) diphenol. The structures of all the synthesised compounds have been analysed using Fourier-Transform Infrared (FT-IR), Nuclear Magnetic Resonance (NMR) spectroscopy, Ultraviolet-Visible (UV-Vis) spectrum, elemental analysis and Powder X-ray diffraction (PXRD). The experimental spectral frequencies of ligand and metal complexes are correlated with theoretically computed vibrational frequencies. The molecular structure of the ligand and its metal complexes has been optimized using B3LYP-6-311G(d,p)/LANL2DZ basis set and their parameters have been discussed. Natural bond orbital and Frontier Molecular Orbital analysis have assessed the presence of a metal-ligand bond in complexes. Further, biological activity studies such as antioxidant, anti-inflammatory, antidiabetic have also been analyzed using various methods. In addition, molecular docking studies have also been performed on all complexes using the α -amylase enzyme structure to calculate the possible binding energy of inhibitors.

© 2021 Published by Elsevier B.V.

1. Introduction

Schiff bases and their metal complexes are extremely utilized in catalytic and the medicinal field due to their greater stability and chelating properties [1]. Similarly, more attention has been focused on the production of transition metal complexes with Schiff bases due to occurrences of N and O donor atoms [2-4]. Transition metal complexes based on the nitro and halogen groups have rich antimicrobial properties. In the past, several researchers suggested that the biological behaviour, e.g., antibacterial, antifungal and antitumor activities, is demonstrated by salicylaldehyde derivatives along with halogen aromatic rings [5,6]. The transition metal complexes provide constant and colored metal complexes with attractive physico-chemical properties, as well as advantageous biological character. Transitional metal complexes binding analysis have recently become the most significant sector in the growth of DNA probes and chemotherapy [7]. In addition, it is also used as sen-

sors for tracking cellular operations in organisms [8]. A Saadeh researcher claimed that several Cu(II) N, O, S-donor chelators have acted as an excellent anticancer agent due to its strong binding capacity among DNA base pairs [9]. Schiff base based on the metal complexes was examined against Gram positive and negative pathogenic microorganisms [10,11]. The transition metal ions such as Co(II), Ni(II) and Cu(II) complexes continue to exist as cofactors in several oxidative enzymes as tyrosinase hydrogenase and lactase [12].

Simple compounds that are associated and interact with DNA usually increase their biological potential. 3d-transition metal complexes are a group of compounds containing metal centre and heteroatoms such as N, O and S, which have been capable of interacting with nucleic acid through the formation of H-bonds [13-15]. Usually, biologically active compounds improve their cleavage activity and thus provide a qualified anti-proliferative agent for various tumor types. Transition metals and ligand integrating this heterocyclic group may undergo a variety of unexpected reactions leading to novel structures and products, several of which are of directly relevant to biological processes [15]. A great deal of importance in the transition metal complexes of 4-Nitro-o-

* Corresponding author.

E-mail address: vennilaindu84@gmail.com (P. Vennila).

phenylenediamine as well as its derivatives has been thoroughly discussed in recent years owing to its unique biological properties and improved DNA binding capabilities. Density Functional Theory (DFT) based on a theoretical calculation of molecular structural properties, HOMO and LUMO are strongly interpreted with the design of the drug molecules. In addition, molecular docking studies have made a significant contribution to the interactions of transition metal complexes between reactive protein target sites that are responsible for antioxidant and biological activity. There is a demand for synthesis of innovative compounds with antimicrobial, DNA-binding and other activity.

Observation of the above-mentioned literature revealed that the Schiff base transition metal complexes were frequently used for pharmaceutical applications. In the present study, an interesting report from the research literature, it is planned to synthesize a few new 3d-transition metal complexes of bis(salicylaldehyde) with Nitro-O-phenylenediamine of Schiff base ligand. Further, molecular characterization, biological activity (such as total antioxidant, anti-inflammatory, anti-diabetic) molecular docking and physicochemical parameters of metal complexes are also discussed with the theoretical calculation.

2. Experimental

2.1. Materials and methods

All chemicals were purchased from Sigma Aldrich (spectroscopic grade) and used without further purification. The elements (C, N and H) were analyzed by Vario EL III CHN type of equipment. The FT-IR spectra of synthesized ligand and its metal complexes were recorded in the region 4000–400 cm^{-1} in evacuation mode using a KBr pellet technique with 1.0 cm^{-1} resolution on a PERKIN ELMER FT-IR spectrophotometer (SAIF, IIT, Chennai, India). The chemical shifts of ^{13}C and ^1H -NMR have been recorded on a Bruker-DRX-400 MHz spectrophotometer using DMSO- d_6 with internal reference as TMS (Sastra university, Thanjavur, Tamil Nadu). The UV-Vis spectra were recorded using a shimadzu 1800 PC spectrophotometer in the range of 200–800 nm using a DMSO solvent (Central Research Laboratory, Erode-Tamil Nadu).

2.1.1. Synthesis of ligand

The Schiff base ligand is prepared with a condensation reaction of 0.1 mol of 4-Nitro-o-phenylenediamine and 0.2 mol of salicylaldehyde blended with 50 ml ethanol and the mixture solution is stirred well with reflux for 2 hours after the mixture slowly turned into yellow precipitate. The precipitate is filtered and washed with distilled water several times. The precipitate is recrystallized using methanol followed by drying at 50°C overnight [16,17].

2.1.2. Synthesis of metal complexes

Three hydrated metal salts ($\text{CoCl}_2 \cdot 6\text{H}_2\text{O}$, $\text{NiCl}_2 \cdot 2\text{H}_2\text{O}$ and $\text{CuCl}_2 \cdot 2\text{H}_2\text{O}$) have been used to synthesize Schiff base metal (II) complexes. Schiff base ligand 0.74 g (3 mol) is separately added with each metal chlorides of 0.18 g of $\text{CoCl}_2 \cdot 6\text{H}_2\text{O}$, 0.10 g of $\text{NiCl}_2 \cdot 2\text{H}_2\text{O}$ and 0.26 g of $\text{CuCl}_2 \cdot 2\text{H}_2\text{O}$ in 20 ml of ethanol solution. After the mixture was well stirred at room temperature colored metal complexes are obtained and the color precipitate is filtrated followed by washing with ethanol, then dried.

2.1.3. Computation study

Vibrational frequency and geometrical optimization calculations of ligand and their complexes were performed by B3LYP-6-311G(d,p)/LANL2DZ [18,19] functional. The optimized structure of ligand and metal complexes have established to the ground state using the absence of imaginary frequency in the force constant method and were predicted without symmetry constraint utilizing

the Gaussian 09W program [20]. The optimized structure is visualized by Gauss view 5.0.8 version. In the Conceptual Density Functional Theory [20], the relationship with total electronic energy (E), the number of electrons (N), ionization energy (I) and electron affinity (A) of quantum chemical descriptors like electronegativity (χ), chemical potential (μ), hardness (η) and softness (σ) at a constant external potential are described with the help of the following formulas.

$$\mu = -\chi = \left[\frac{\partial E}{\partial N} \right]_{v(r)} = -\left\{ \frac{I+A}{2} \right\} \quad (1)$$

$$\eta = \frac{1}{2} \left[\frac{\partial^2 E}{\partial N^2} \right]_{v(r)} = \left\{ \frac{I-A}{2} \right\} \quad (2)$$

$$\sigma = \frac{1}{\eta} \quad (3)$$

It is required to measure the ionization energy and electron affinity values for determining the experimental values of hardness and chemical potential. On the other hand, Koopmans Theorem [21], which is a bridge between Conceptual Density Functional Theory and Molecular Orbital Theory can be used for the approximate prediction of ionization energy and electron affinity values of molecules. According to this theorem, the negative values of energies of HOMO and LUMO orbitals of any molecule correspond to its ionization energy and electron affinity, respectively. In this way, the aforementioned quantum chemical parameters are calculated using frontier orbital energies. To describe the electrophilic power of chemical species, in 1999, Parr, Szentpaly and Liu [22] modelled electrophilicity index (ω) based on electronegativity (or chemical potential) and hardness of chemical species via the following formula. Then Chattaraj defined the nucleophilicity (ε) is the multiplicative inverse of electrophilicity index.

$$\omega = \frac{\chi^2}{2\eta} = \frac{\mu^2}{2\eta} \quad (4)$$

$$\varepsilon = \frac{1}{\omega} \quad (5)$$

Polarizability (α) is another reactivity descriptor and it is calculated depending on diagonal components of polarizability tensor.

$$\bar{\alpha} = 1/3[\alpha_{xx} + \alpha_{yy} + \alpha_{zz}] \quad (6)$$

Addition, the second order-perturbative energies of Co(II), Ni(II) and Cu(II) complexes obtained from the natural bond orbital analysis (NBO) [23,24] have been used in elucidating of the intramolecular interactions.

2.2. Biological study

2.2.1. Total antioxidant activity

The total antioxidant properties of the title metal complexes were calculated by the method of prito *et al.* [25].

2.2.2. Antidiabetic activity

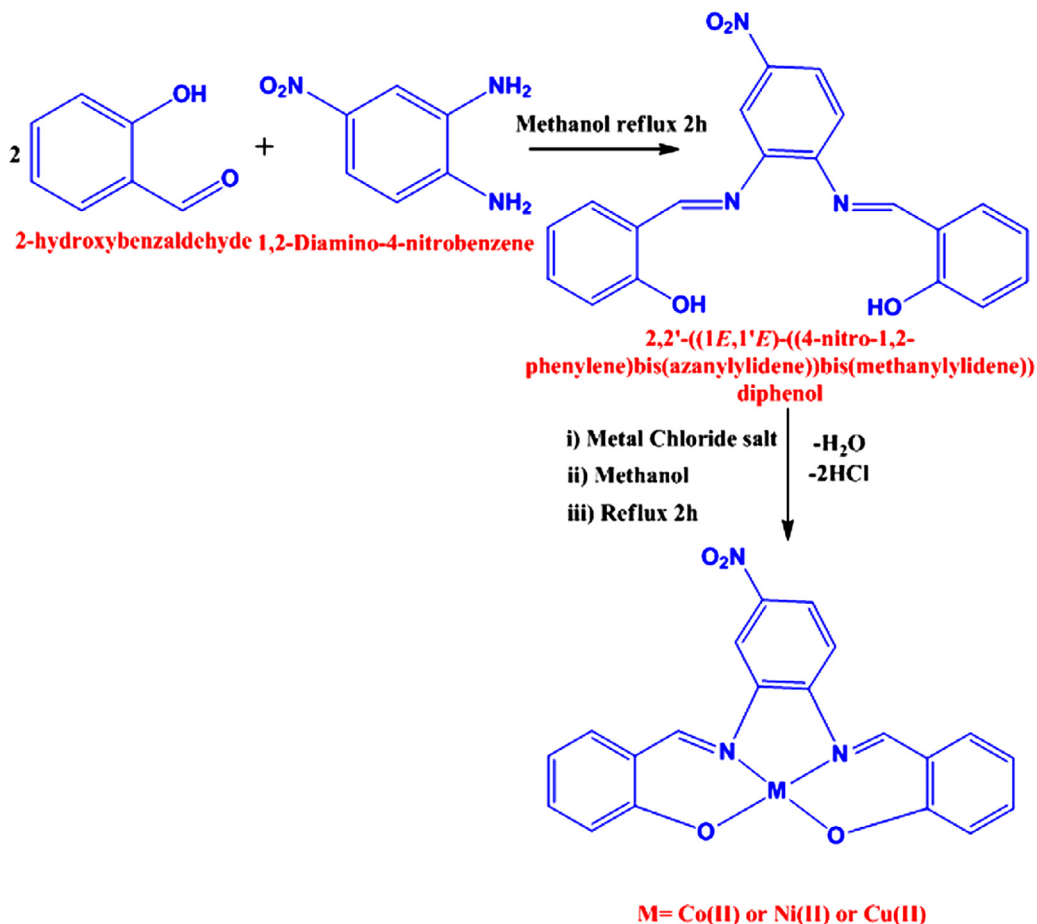
The antidiabetic activity was performed using the appha amylase method [26]. The procedures are given in supplementary material.

2.2.3. Anti-inflammatory activity (BSA denaturation technique)

The *in vitro* anti-inflammatory behaviour of metal complexes was investigated via bovine serum albumin (protein denaturation technique) [27]. The procedures are given in supplementary material.

Table 1
Physical data and elemental analysis of the ligand and metal complexes.

Compound	Molecular formula	Colour	M.Pt (°C)	Elemental analysis (%)			Found (Cal.) (Metal %)	Molar conductance
				C	H	N		
Ligand	C ₂₀ H ₁₅ N ₃ O ₄	Yellow	361	66.48	4.19	11.83	-	-
Cobalt complex	C ₂₀ H ₁₃ CoN ₃ O ₄	Brown	489	49.21	2.78	8.69	12.16	11.14
Nickel complex	C ₂₀ H ₁₃ NiN ₃ O ₄	Light green	488	49.13	2.81	8.59	12.00	12.21
Copper complex	C ₂₀ H ₁₃ CuN ₃ O ₄	Green	493	48.85	2.65	8.51	12.88	14.48



Scheme 1. Synthetic route of Schiff base ligand and its metal complexes.

2.2.4. Molecular docking

The molecular docking studies are performed using HEX 8.0 software. The three-dimensional structure of the title compounds was built by using Chem Bio 3D ultra 13.0 software and is minimized by MM2 with a maximum number of 5000 iterations and a minimum RMS gradient of 0.10. Crystal protein structure (PDB ID: 1HNY.pdb) were obtained by Protein Data Bank (www.rcsb.org) and docked molecules imaged by discovery studio 4.1 [28].

3. Results and discussion

The percentage of elemental analysis of ligand and metal complexes is well associated with the suggested structure [29,30]. The title metal complexes and neutral Schiff base ligand were thermally stable (room temperature) and soluble in DMF and DMSO, though partly soluble in alcohol. The percentage of CHN data, physical data and molar conductance for synthesized compounds are tabulated in Table 1. The proposed structure of Cobalt, Nickel and Copper metal complexes are illustrated in Scheme 1.

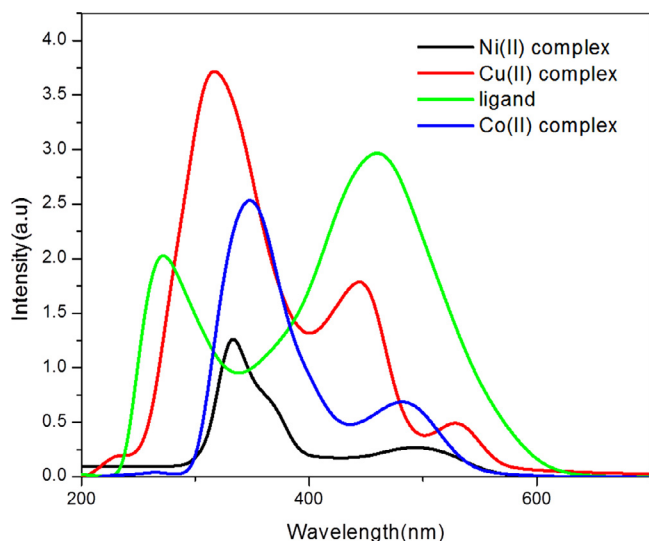
3.1. Electronic spectra

The observed electronic spectra of the ligand and its metal complexes were recorded in DMSO solutions at 200–800 nm ranges [29]. Electronic spectra of the metal complexes are closely interpreted with ligand and shown in Fig. 1. The absorption bands of the Schiff base ligand vary with their metal complexes which revealed that ligand coordination with the metal ions. The Schiff base ligand, displayed two strong absorption bands at 284 and 478 nm were attributed to $n \rightarrow \pi^*$ and $\pi \rightarrow \pi^*$ electronic transitions respectively. Consequently, the electronic spectra of Co(II) complex appeared in medium intensity bands at 336, 389, 496 nm were attributed to $\pi \rightarrow \pi^*$, $L \rightarrow M$ (LMCT), ${}^4A_{2F} \rightarrow {}^4T_{1P}$ transitions, indicating that less-spin distorted tetrahedral geometry. Similarly, the magnetic moment value of the Co(II) complex was determined to be 3.88 B.M. and is also responsible for the predicted distorted tetrahedral geometry [15,30]. Further, electronic absorption spectra of Ni(II) complex are observed three absorption bands at 332, 384 and 492 nm due to $\pi \rightarrow \pi^*$, $L \rightarrow M$ (LMCT), ${}^1A_{1g} \rightarrow {}^1A_{2g}$ transitions, respectively [29,30]. Likewise, Ni(II) complex exhibits a magnetic

Table 2

Calculated energies, dipole moments (μ), maximum absorption wavelengths (λ_{\max}), excitation energies (eV), oscillator strengths (f), assignment of electronic transitions (HOMO(H) \rightarrow LUMO(L)) and major contribution (%) for the metal complexes and ligand in DMSO solvents.

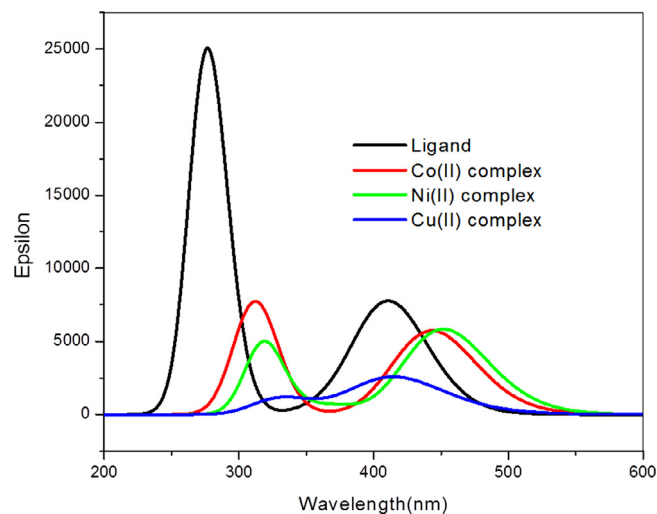
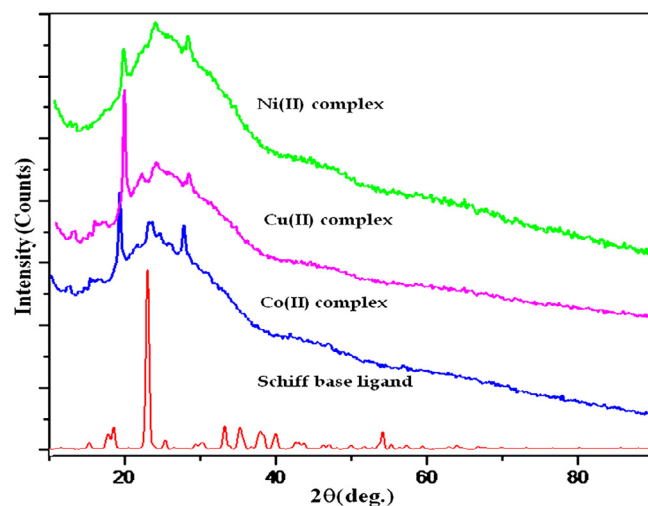
Ligand & complexes	Parameters						
	E_{total} (a.u)	Dipole moment	λ_{\max}	f	Transition energy	Electronic transition	Major % contribution
Ligand	-	6.552	286.48	0.3024	2.6475	H \rightarrow L	94.60%
	1236.23		476.52	0.1436	2.9938	H-1 \rightarrow L	95.26%
Cobalt complex	-	5.293	310.59	0.1984	1.8193	H \rightarrow L	94.38%
	2300.42		452.18	0.0129	2.0314	H-1 \rightarrow L	95.62%
Nickel complex	-	2.714	313.48	0.2817	2.1936	H \rightarrow L	93.35%
	2325.22		458.66	0.0146	2.2886	H-1 \rightarrow L	94.24%
Copper complex	-	5.131	324.66	0.4434	2.8556	H \rightarrow L	95.26%
	2351.39		498.84	0.0109	3.0143	H-1 \rightarrow L	96.39%

**Fig. 1.** Electronic spectra of metal complexes and Schiff base ligand.

moment value of zero B.M., which indicates a square planar geometry [31]. Additionally, the absorption bands of Cu(II) complex existed at 318, 444, 528 nm were assigned to $\pi \rightarrow \pi^*$, L \rightarrow M (LMCT), $^2B_1g \rightarrow ^2A_1g$ transitions and magnetic moment value was found to be 1.86 B.M., which suggests that the Cu(II) complex had a square planar geometry [15,30,32]. In addition, the calculated dipole moment (μ), wavelength maxima (λ_{\max}), electronic transition, atomic orbital major contribution, oscillator strength (f) and absorption energy (E) are shown in Table 2. The calculated strong absorption bands were found to be 476.52 nm for Schiff base ligand, 452.18 nm for Co(II) complex, 458.66 nm for Ni(II) complex and 498.84 nm for Cu(II) complex and are shown in Fig. 2. The results suggesting that electrons occurred from EHOMO to ELUMO transition (95.26, 95.62, 94.24 and 96.39 % orbital contribution).

3.2. Powder X-ray diffraction (XRD) study

Powder X-ray diffraction peaks of title compounds were observed in the range of $2\theta = 10-90^\circ$ using XPERT-3 diffractometer at 25°C [33]. While single crystal X-ray crystallography is the most reliable source of information on the structure of the complex, the difficulty of obtaining appropriate crystals in the correct symmetrical form has made this approach unsuitable for such a study. During the powder X-ray diffraction study (Fig. 3) showed, only Cu (II) complexes displayed sharp peaks, although no peaks were seen for the rest of the complexes suggesting their amorphous existence. A comparison of ligand diffractograms and complexes revealed the crystalline nature of the complex. The average grain size of the complexes was calculated using the Debye Scherer equation. The

**Fig. 2.** Calculated UV-Vis absorption bands of metal complexes and Schiff base ligand.**Fig. 3.** Powder X-ray diffraction of ligand and metal complexes.

Co^{2+} , Ni^{2+} and Cu^{2+} complexes and ligand comprise an average crystalline size of 24.1 nm, 42.3 nm and 28.4 nm and 59.6 nm, respectively.

3.3. Vibrational spectra

Vibrational study on the basis of both experimental and theoretical approaches provides a detailed understanding of the nature of functional groups, the evaluation of structural changes and

Table 3
Assignments of fundamental vibrations of metal complexes.

S. no.	Metal complexes/ Functional group	Copper complex		Nickel complex		Cobalt complex	
		Exp.	Scaled	Exp.	Scaled	Exp.	Scaled
1	ν CH	3154	3088	3211	3094	3076	3115
2	ν NC	1644	1629	1613	1668	1626	1659
3	β NC	865	908	815	912	806	854
4	ν ON	1341	1356	1412	1436	1337	1362
5	ν C=C	1441	1482	1496	1463	1458	1469
6	ν OC	1031	1044	996	1021	964	985

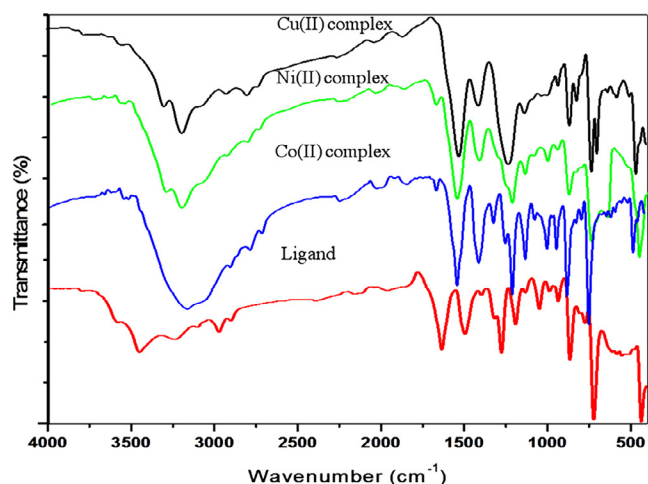


Fig. 4. Experimental FT-IR spectra of metal complexes and Schiff base ligand.

the prediction of their spectral characteristics. The experimental and theoretically calculated vibration spectra of title compounds are shown in Fig. 4 and S1. The observed (O-H stretching frequencies) vibrational spectra of ligand showed large bands at 3512, 3429 cm^{-1} , which are correlated well with calculated bands of 3440 and 3438. In the present study, experimentally observed C-H vibrational bands of ligand have appeared in the ranges 3158–2846 cm^{-1} whereas the calculated vibration bands were assigned to 3145–2878 cm^{-1} (refer supplementary material in Table S1).

The observed C-N stretching frequencies of ligand are assigned at 1672, 1654 cm^{-1} , which also agreed with calculated bands of 1655 and 1642 cm^{-1} . The coordination of metal through the N and O atoms of aromatic ring cause significant changes in the bands arrived for ligand after the complexation, which was evident from IR bands of both ligand and metal complexes [32–35]. The metal complexes sharp absorption frequencies appeared at 1644 (Cu(II)), 1613 (Ni(II)) and 1626 (Co(II)) cm^{-1} , which are also correlated with calculated bands. Similarly, C-N bending vibrational frequencies are assigned at 865 (Cu(II)), 815 (Ni(II)) and 806 cm^{-1} (Co(II)), which correlated well with calculated bands (Table 3). The observed medium C-C stretching vibrational band appeared at 1441 (Cu(II)), 1496 (Ni(II)) and 1458 (Co(II)) cm^{-1} . Further, the experimental N-O stretching vibrational frequencies arrived at 1341 (Cu(II)), 1412 (Ni(II)) and 1337 (Co(II)) cm^{-1} . It is noted that the band moved towards the lesser frequency after its complexation.

3.4. NMR spectra

The NMR spectroscopy are powerful tools for the direct detection of chemical species and forms of molecular interactions in complex materials. The NMR spectral analysis provided a comprehensive account that was considered to be suitable for the assignment of protons (^1H) and carbon (^{13}C). Commonly, the aromatic

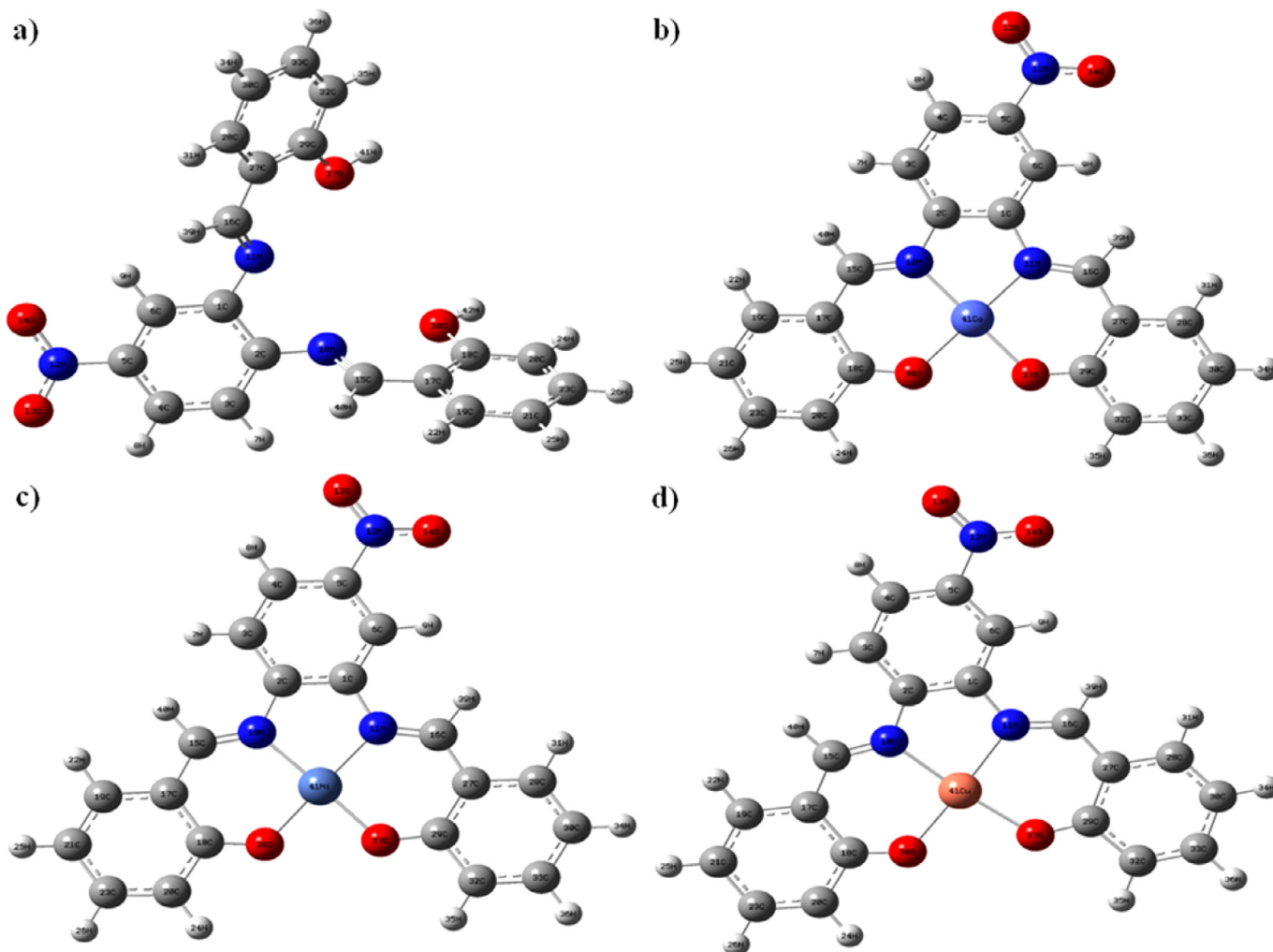
compound of chemical shifts isotropic carbons is obtainable in the range of 100–160 ppm. The ^{13}C and ^1H NMR spectra of Schiff base ligand are shown in Fig.S2 and S3. The ^{13}C and ^1H NMR spectra of ligand is calculated by B3LYP functional/6-311++G (2d,p) basis set, which quite agreed with experimental NMR spectra shown in Table 4. In this analysis, ^{13}C chemical shift aromatic carbon (C5) is detected at 158.2 ppm due to increased electronegativity of the NO_2 group assigned to the aromatic ring. The observed ^{13}C chemical shifts of aromatic ring carbons arrived at C29 (138.5), C18 (136.9), C1 (135.8), C6 (128.4), C32 (127.6), C28 (123.4), C19 (122.5), C33 (118.8), C33 (119.3), C27 (119.6), C17 (118.2), C4 (121.6), C21 (123.4), C3 (126.8) and C20 (119.2) ppm were in quite agreement with the theoretically calculated chemical shifts. The aliphatic carbon C15 and C16 chemical shift are obtained at 55.4 and 61.5 ppm. The results (Table 4) are clearly shown that the electronegative assets polarizing of O and N have influenced the distribution of the electron adjacent carbon atoms, which have decreased electron density as well as chemical shifts are appeared in higher down filed values. Similarly, H39 and H40 proton chemical shifts are arrived at 8.6 and 8.4 ppm, respectively. Additionally, H41 and H42 proton chemical shifts found to be 3.4 and 2.9 ppm and also coincide with calculated values.

3.5. Geometrical parameters

The applicable geometrical parameters of metal complexes and neutral ligand are numbered according to the convention shown in Fig. 5. The physic-chemical parameter of bond length, bond angle and dihedral angles of title compounds are presented in (supplementary material) Tables S2–S5. The theoretically calculated (ligand) bond lengths of N-O ≈ 1.29 (1.28 Å), C=N ≈ 1.29 (1.28 Å), C-N ≈ 1.39 (1.42 Å), C-O ≈ 1.37 (1.34 Å), O-H ≈ 0.99 (0.97 Å) slightly deviate (RMSD ≈ 0.95 Å) from the literature data [17,33 and 34]. The important bond length (C-N and C-C) of metal complexes M-O and M-N (Metal(M)) have slightly deviated than ligand (refer Table S2–S5 supplementary material) due to some amount of charge transferred metal ion to ligand (ligand coordinated to metal ion). This result also accords with the prediction of IR and NMR spectra. In Co(II) complex, the bond length of Co41-O38, O37-Co41, N11-Co41, N10-Co41 are 1.90 (2.11°), 1.91 (2.06°), 1.93 (1.98°), 1.91 (1.96°), respectively. The bond angles of O38-Co41-N10, O37-Co41-O38, N11-Co41-N10, N11-Co41-O37 are 104.9 (110.5°), 85.4 (90.6°), 110.5 (108.9°), 94.6 (91.4°) respectively. Similarly in Ni(II) complex, the bond length of Ni41-N10, N11-Ni41, Ni41-Co37, Ni41-Co38 are 1.87 (1.85°), 1.88 (1.86°), 1.83 (1.84°), 1.84 (1.83°), respectively. The bond angle of N10-Ni41-N11, N10-Ni41-N11, O38-Ni41-O37, N11-Ni41-O37 are 108.3 (114.8°), 111.8 (110.9°), 86.9 (90.4°), 98.4 (92.6°), respectively. Further, in Cu(II) complex, O38-Cu41, N10-Cu41, N11-Cu41, O37-Cu41 are 1.94 (1.91°), 1.99 (1.92°), 2.03 (1.93°), 1.99 (1.94°), respectively. The bond angle of O38-Cu41-N10, N11-Cu41-N10, N11-Cu41-O37, O37-Cu41-O38 are 108.3 (11.8°), 109.2 (115.4°), 94.8 (90.5°), 88.45 (91.4°), respectively. The calculated bond angles of the metal complexes and the neu-

Table 4
¹H & ¹³C NMR spectral data of Schiff base ligand.

Atoms	Experimental chemical shift (σ) ppm	B3LYP/6-311+G(2d,p) GIAO	Atoms	Experimental chemical shift (σ) ppm	B3LYP/6-311+G(2d,p) GIAO
C5	158.2	154.43	C15	55.4	64.9
C29	138.5	139.9	C16	61.5	76.9
C18	136.9	138.1	H39	8.5	8.6
C1	135.8	137.1	H40	8.3	8.4
C2	136.4	135.5	H8	7.2	6.9
C6	128.4	132.5	H9	7.4	6.7
C32	127.6	128.3	H31	7.5	6.1
C28	123.4	118.9	H22	7.6	6.0
C19	122.5	118.5	H26	6.9	5.9
C23	118.8	114.0	H36	6.6	5.8
C33	119.3	113.5	H34	6.4	5.6
C27	119.6	119.0	H25	6.2	5.6
C17	118.2	118.9	H7	5.8	5.4
C4	121.6	115.8	H24	6.4	4.8
C21	123.4	103.9	H35	5.9	4.7
C30	123.9	103.9	H42	3.4	3.6
C3	126.8	120.8	H41	2.9	3.5
C20	119.2	115.4	-	-	-

**Fig. 5.** Optimized molecular structure (a) Schiff base ligand (b) Cobalt complex (c) Nickel complex and (d) Copper complex.

tral ligand are close to the values of literature and the slightly deviated is approximately 0.98 Å (RMSD). Additionally, the dihedral angles of the metal complexes and the neutral ligand indicate that the fragment does not have the same plane as the rest of the complex.

3.6. Frontier molecular orbitals

Some electronic structure principle called as Maximum Hardness Principle [36], Hard and Soft Acids Bases Principle [37], Minimum Electrophilicity Principle [38], Minimum Polarizability Prin-

Table 5
Quantum Chemical Parameters of Cobalt, Nickel and Copper complexes at B3LYP/6-311G(d,p)/LANL2DZ.

Parameters	Schiff base ligand	Cobalt complex	Nickel complex	Copper complex
HOMO (-I)	-5.97	-9.63	-9.64	-9.75
LUMO (-A)	-2.27	-8.71	-8.43	-8.49
ΔE (L-H)	3.70	0.92	1.21	1.27
$\mu = -(I+A)/2$	-4.12	-9.17	-9.04	-9.12
$\eta = (I-A)/2$	1.85	0.46	0.61	0.63
$\omega = \mu^* \mu / 2\eta$	4.59	90.88	67.33	65.66
$\Delta N_{max} = -\mu/\eta$	2.23	19.82	14.90	14.40
α (au)	299.99	494.25	395.59	508.15
DM (debye)	9.41	3.94	6.12	3.33
DE (a.u)	-1236.18	-2300.36	-2325.17	-2351.33

principle [39] and Minimum Magnetizability Principle [40] in the literature provide useful information about stability or reactivity of molecules. Chemical hardness is defined as the resistance to charge transfer of chemical species. HSAB theory suggests that "hard acids tend to coordinate hard bases and soft acids tend to coordinate soft bases." According to Maximum Hardness Theorem, chemical hardness is a prerequisite for consistency and hard molecules are more stable compared to soft ones. In the hard and soft classification of Pearson, Co^{2+} , Ni^{2+} , Cu^{2+} ions appear among borderline acids. Experimental hardness values of these ions obey the order: $Cu^{2+} > Ni^{2+} > Co^{2+}$ [40,41]. In our calculations, we obtained the same order. It is apparent from the data given in the related table that the ligand considered in this study is harder than the aforementioned ions. If so, one can say that the ligand interacts more powerful with Cu^{2+} ion. Already, hardness value of Copper complex is higher than that of others and this complex is more stable compared to Nickel and Cobalt complexes (refer Table 5).

Minimum Electrophilicity Principle and Minimum Polarizability Principle have been suggested by inspiring from Maximum Hardness Principle. Minimum Electrophilicity Principle states that in an exothermic reaction, sum of the electrophilicity values of products should be smaller than that of reactants. It can be understood from this information, electrophilicity can be also used in reactivity analysis of molecules. Stable molecules should have lower electrophilicity values compared to reactive molecules. If so, Minimum Electrophilicity also confirms the stability of Copper complex. According to the Minimum Polarizability Principle, in a stable state, polarizability is minimized. It is important to note that the relation between polarizability and softness has been proven by Ghanty and Ghosh. Minimum Polarizability Principle and the polarizability data given in the related table imply that Nickel complex will be more stable compared to others. This result is not compatible with experimental observations and the results of Maximum Hardness and Minimum Electrophilicity Principles. It is well known that there is a remarkable correlation between dipole moment and polarizability. Some researchers noted that dipole moment is a measure of polarizability. The molecules having high dipole moment values are more polarizable [42]. One can say that dipole moment values also support the stability of Copper complex.

Fig. 6 presents the frontier molecular orbital densities and MEP plots of the Ligand and three metal complexes [43]. For the ligand molecule, the EHOMO density as an indicator of the nucleophilic attack site is expanded over on the whole surface, except for the oxygen atom of the nitro group. Also, the ELUMO density depicting the electrophilic attack site is mainly distributed over the whole surface and partly on the benzylic group that connects the two (E)-2-((methylimino) methyl) phenol rings. The EHOMO and ELUMO amplitudes show over the L-M complex in a different distribution from each other. For instance, the EHOMO density of the cobalt complex distributes over the surrounding of the center of the Co-chelating while the EHOMO of the nickel complex has positioned on the whole surface except for the $-NO_2$ group. Also,

MEP plots obtained from the total SCF (self-consistent-field) density clearly represent the electron-rich and electron-poor region based on the electrostatic potential. As expected, the surrounding of the oxygen and nitrogen atoms are the red color demonstrating the electron-rich field having the highest negative electrostatic potential value. And the hydrogen atoms of the hydroxy group are the blue color implying the electron-poor regions having the highest positive electrostatic potential value. The presence of the metal atom in the molecule influences the distribution of the electron density: all-metal complexes mainly show the green-blue color all over their surfaces. Here, the electrostatic potential value has been determined as $Cu(II) (\pm 0.778e) > Ni(II) (\pm 0.353e) > Co(II) (\pm 0.214e)$ that support the tendency of the antioxidant activity of these complexes.

3.7. Natural bond orbitals

The NBO analysis was performed for predicting the existence of the donor-acceptor interaction on the molecule [44], and the results were presented in supplementary material Table S6. Due to the existence of the unsaturated rings, the resonance interactions are mainly contributed to the stabilization of the ligand and its metal complexes in addition to the cieplak interactions predicted for the metal complexes [23, 24]. For the ligand, the lone pair electron of the oxygen atoms of the hydroxyl group has a main role in contributing to the stabilization energy; the stabilization energy of the interactions $LP(2) O37 \rightarrow \pi^*C29-C32$ and $LP(2)O38 \rightarrow \pi^* C18-C20$ are calculated as 32.68 and 32.79 kcal/mol, respectively. If the MEP plot of the Ligand molecule is recalled, the surrounding of the oxygen atoms is in red color. On the other hand, the presence of the Co, Ni, and Cu metals in the center of the molecule provides the complexes more electrophilicity. For the Copper complex, the interactions $\pi C20-C23(2) \rightarrow \pi^*C18-O38$ and $\pi C3-C4(2) \rightarrow \pi^*C2-N10$ have greatly supported the stabilization with the energies of 25.23 and 22.67 kcal/mol. Addition, $\pi C17-C19(2) \rightarrow \pi^*N10-C15$, $\pi C21-C23(2) \rightarrow \pi^*C17-C19$, and $LP(2) O38 \rightarrow \pi^*C18-C20$, 48.01, 32.67, and 30.83 kcal/mol. For the Nickel complex, the stabilization energy of the interactions $\pi C17-C19(2) \rightarrow \pi^*N10-C15$, $\pi C21-C23(2) \rightarrow \pi^*C17-C19$, and $LP(2) O38 \rightarrow \pi^*C18-C20$ are found to be in 48.01, 32.67 and 30.83 kcal/mol, respectively. For the Cobalt complexes complex, the resonance interactions have quite provided the stabilization, $E(2)$ of the interactions for $\pi C1-N11(2) \rightarrow \pi^*C16-C27$, $\pi C2-N10(2) \rightarrow \pi^*C15-C17$, $\pi C3-C4(2) \rightarrow \pi^*C1-N11$, $\pi C20-C23(2) \rightarrow \pi^*C18-O38$, $\pi C32-C33(2) \rightarrow \pi^*C29-O37$ are calculated as 29.08, 29.63, 30.39, 28.48, and 28.28 kcal/mol.

3.8. Natural population analysis (NPA) and Metal-Ligand charge interaction analysis

The transfer of charges acting a vital role in applying quantum chemical calculations to molecular system due to atomic charges affecting the dipole moment, polarization, molecular nature (acid-

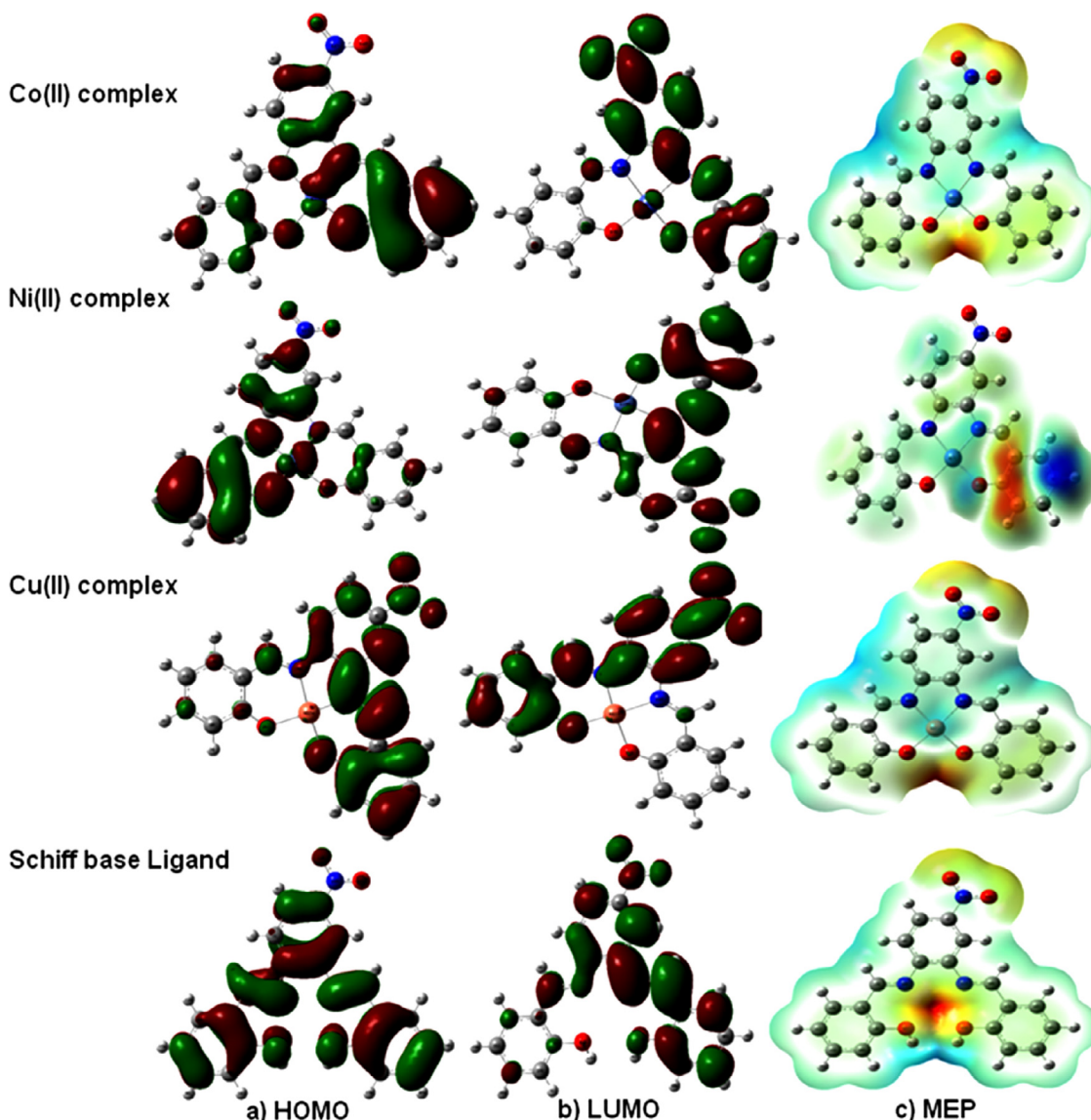


Fig. 6. a) HOMO, b) LUMO (isoval: 0.02) and c) MEP (iso value: 0.0004) plots of the Schiff base ligand and metal complexes using the B3LYP/6-311G(d,p)/LANL2DZ basis set.

ity and basicity) and such other properties of the molecular system [45]. Furthermore, the electron interaction between ligand to metal could be predicted by NPA. Natural atomic charges (NAC) were determined earlier in experimental section. The presence of both N and O as ligand coordinated atoms allows enriching the Schiff base electron donation tendency. The NAC and valence electron configurations of the ligand and complexes with half the symmetry details are shown in Table 6 [45 and 46]. The calculated NAC of Co, Ni and Cu ions are observed as 0.3124, 0.4428 and 0.7673, respectively and are considerably below than formal charge (+2). The results show that, since negative electron density is being transferred from the ligand, the atomic charge of metal ions could be reduced. From the observation, the significant amount of charge transferred occurred from metal to ligand have been identified.

3.9. Thermodynamic parameters

Metal-ligand stability constants were calculated using Half Integral & Graphical procedure and the values are shown in supplementary material Table S7. The Co(II), Ni(II) and Cu(II) complexes of the representation Schiff base ligand were chosen for the eval-

uation of the metal-ligand constant stability at 35 and 45°C in ethanol-water (75:25%) medium and at constant ionic strength at $\mu=0.1$ M (NaNO₃). While temperatures rise, the value of metal ligand stability constant decreases, indicating that low temperature is favourable for complex formation [47]. Mean stability constant values were observed to decrease with growing ion intensity in all cases and to demonstrate a diminishing trend with rising temperatures. The thermodynamic parameters (ΔH , ΔG and ΔS) have been estimated and are given in supplementary material Table S8. In addition, $\log(K)$ values decrease with an increase in complexing temperature. The negative values of ΔG indicated spontaneous reactions between metals and ligand and negative values of ΔH demonstrated the exothermic existence of the interaction between metal and ligand. Further, the positive ΔS values suggest that the entropy effects is considered to also be predominant over enthalpy effect. In the structures of analysis, Schiff base ligand acts as a donor species and metal ion acts as an acceptor. Co(II), Ni(II) and Cu(II) with unoccupied d orbitals (d^7 , d^8 , d^9 system) have a capacity to accept π -donation from Schiff base ligand, while Co(II) complexes also with lowest electron at d orbital have a higher constant formation than other metal complexes. The results have

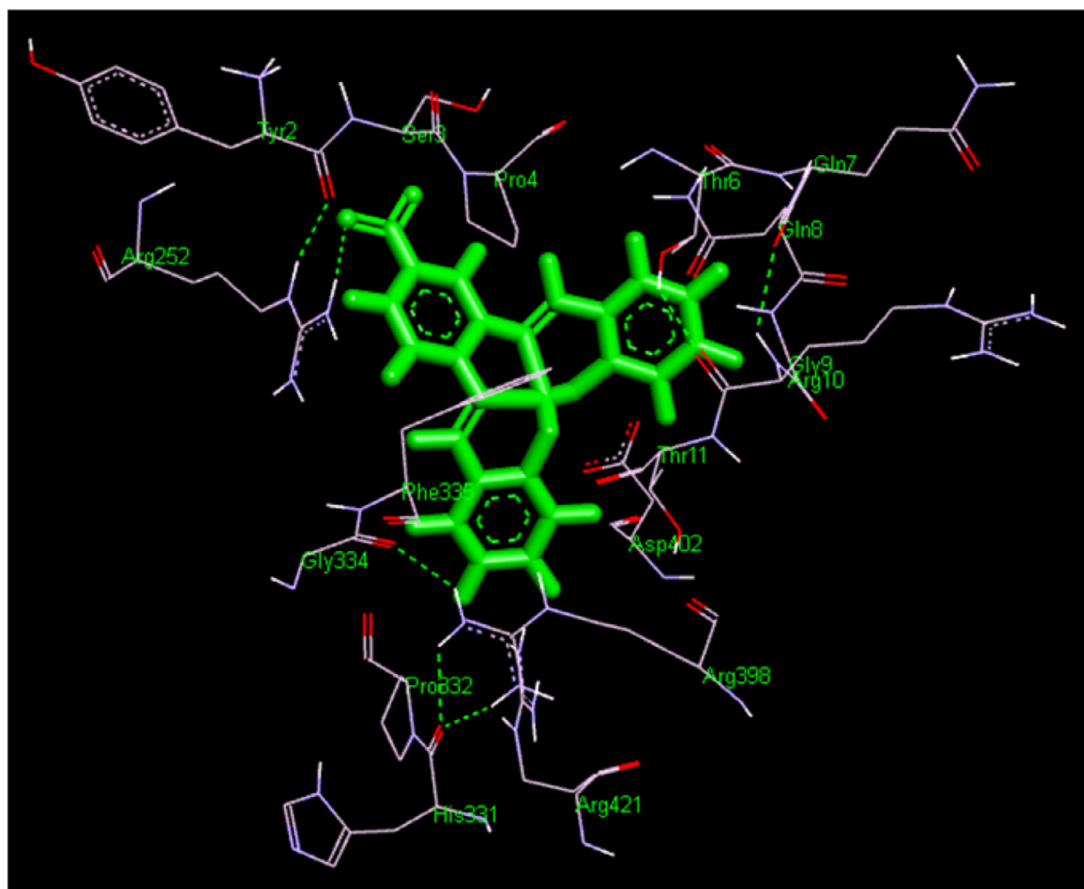


Fig. 7. Molecular docking interaction of cobalt complex with α -amylase (1HNY.pdb).

Table 6

Natural Atomic charges and electron configurations from the natural population analysis (NPA) of title compounds.

Compounds	Atoms	Natural charge	Natural electron configuration
Ligand	N11	-0.5452	[core]2S(1.40)2p(2.97)3p(0.01)
	N12	-0.5509	[core]2S(1.09)2p(3.41)3p(0.03)
	O37	-0.6979	[core]2S(1.71)2p(4.95)3p(0.01)
	O38	-0.6998	[core]2S(1.77)2p(4.86)3p(0.01)
Cobalt complex	N11	-0.6321	[core]2S(1.29)2p(4.10)3p(0.01)
	N12	-0.6244	[core]2S(1.25)2p(3.81)3S(0.01)
	O37	-0.6865	[core]2S(1.63)2p(4.82)3p(0.01)
	O38	-0.6984	[core]2S(1.63)2p(4.85)3p(0.01)
Nickel complex	Co41	0.3124	[core]4S(0.37)3d(7.19)4p(0.78)5p(0.01)
	N11	-0.7136	[core]2S(1.26)2p(4.17)3p(0.01)
	N12	-0.7128	[core]2S(1.21)2p(3.69)3S(0.01)
	O37	-0.5506	[core]2S(1.66)2p(4.85)3p(0.01)
Copper complex	O38	-0.5473	[core]2S(1.65)2p(4.85)3p(0.01)
	Ni41	0.4428	[core]4S(0.40)3d(8.04)4p(0.73)
	N11	-0.4608	[core]2S(1.29)2p(4.17)3p(0.02)
	N12	-0.4691	[core]2S(1.07)2p(3.41)3S(0.01)3p(0.03)
	O37	-0.6068	[core]2S(1.66)2p(4.86)3p(0.01)
	O38	-0.6163	[core]2S(1.66)2p(4.91)3p(0.01)
	Cu41	0.7673	[core]4S(0.38)3d(9.02)4p(0.58)5p(0.01)

shown that formulation constant for Cu(II) is greater than the Ni(II) complex, which could be attributable towards its positive energy distribution and ligand deformation geometry. The stability of the metal complexes follows a trend: Co(II) > Ni(II) > Cu (II).

3.10. Biological study

3.10.1. In vitro antioxidant activity (Phosphomolybdenum method)

Antioxidant activity of the Schiff base ligand and metal complexes concerning *Ascorbic acid* and compared in various concen-

trations (50–500 mM) [48 and 49] and antioxidant activities observation values illustrated in Fig.S4 (refer Table S9 supplementary material). The percentage of inhibition of complexes are compared with control and are given the following order *Ascorbic acid* > Cu(II) > Ni(II) > Co(II). The results of Schiff base ligand, Nickel and Cobalt complexes showed almost nearer performance to the standard at concentrations of 50–500 mM and Nickel and Copper complexes have higher antioxidant than Cobalt complexes complex but lower than *Ascorbic acid*. The results suggested that Nickel and Copper complexes have very good antioxidant activity. The oxidiz-

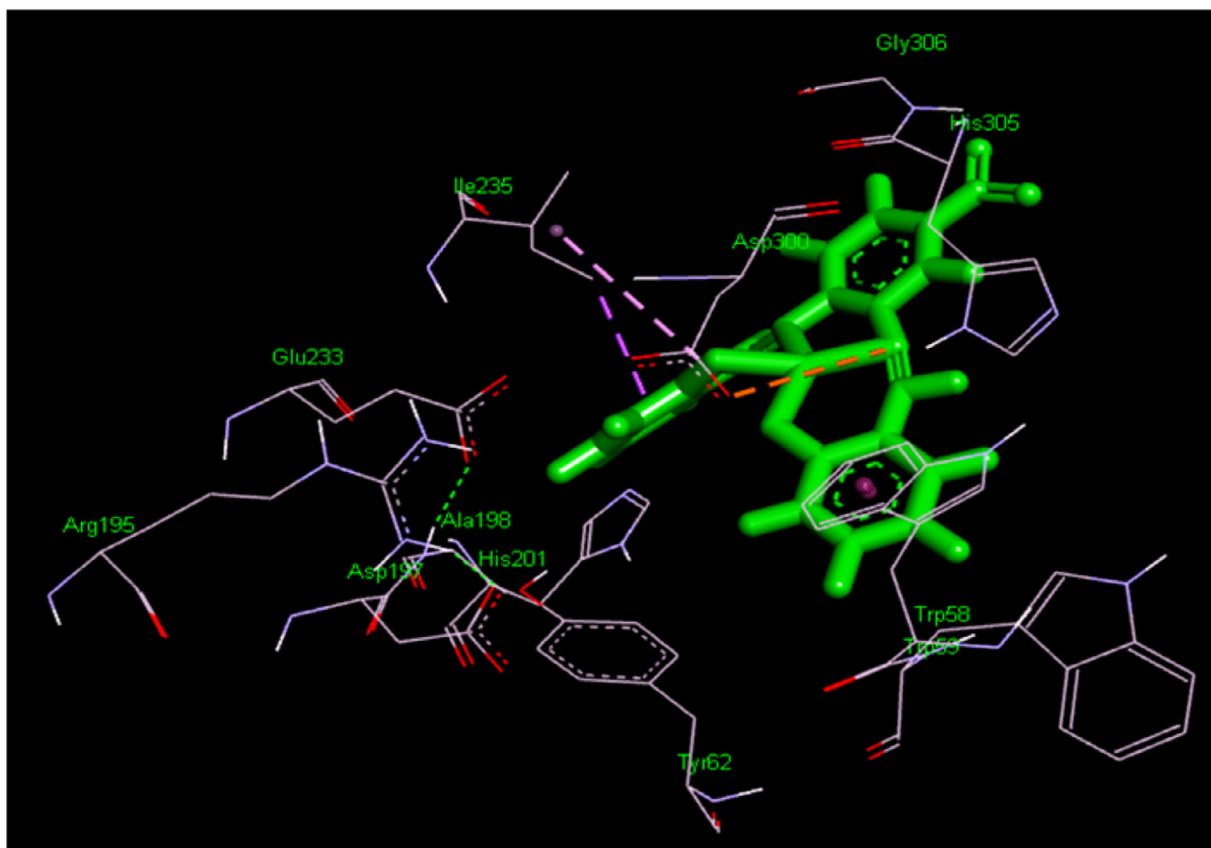


Fig. 8. Molecular docking interaction of Nickel complex with α -amylase (1HNY.pdb).

ing ability of metal complexes is correlated with the presence of compounds to exercise action by splitting the free radical chain by contributing hydrogen atoms. The results provide a link to the use of the title complexes in the treatment of pathological diseases caused by oxidative stress.

3.10.2. Antidiabetic activity

The α -amylase enzymes are involved in the digestion of carbohydrates which are broken down into glucose units. The inhibition activity of α -amylase has been investigated for the reduction of postprandial blood glucose levels, a therapeutic target for diabetic conditions. The title complexes antidiabetic activities were analyzed with α -amylase enzyme inhibition (various concentrations 50, 100, 200, 250, 500 mM) (refer Table S10 supplementary material) and the results are represented in Fig.S5. The results showed that the Copper complex could have better performance than Nickel and Cobalt complexes and the variation antidiabetic activities are due to the nature of the metal ions [26].

3.10.3. Anti-inflammatory activity

The human body defends itself against pathogens, allergens, burns, poisonous substances and other *nociceptive stimuli*, and several of them are chronic pathogens. The Schiff base metal complex has a rich anti-inflammatory ability and is widely used to prevent inflammation. The anti-inflammatory activity of the title complexes were analyzed at different concentrations of 50 μ g/mL, 100 μ g/mL, 200 μ g/mL, 250 μ g/mL and 500 μ g/mL using the Bovine Serum Albumin (BSA) denaturation technique, while diclofenac sodium was used as a reference drug. The percentages of inhibition are shown in Fig.S6. The Cobalt, Nickel and Copper complexes showed effective anti-inflammatory activity compared to the diclofenac sodium

drug and also an excellent percentage of inhibition (see Table S11 supplementary material), which is almost equal to the standard diclofenac sodium drug [50].

3.10.4. Molecular docking study with α -amylase

Molecular docking studies are an important tool for computer-aided drug design and have further attempted to determine the structural mode of the active sites of the receptors through their various cellular functional interactions [51]. The docking studies are very useful for predicting the ability of the Schiff base of studied metal complexes to bind to α -amylase enzyme (1HNY.pdb) and to explain an interesting new therapeutic target for antidiabetic activity. In the present study, Schiff base metal complexes are shown to have a good bonding interaction with the active site and the results are given in Table 7 and Figs. 7-9. The binding energies of Cobalt complex as -291.83, Nickel complex as -287.43 and Copper complex as -296.54KJ/mol were identified, whereas the Copper complexes showed strong hydrogen bonding to amino acid residues of 1HNY [51]. In addition, two forms of hydrogen bonding interaction are observed in the case of the Copper complex, azomethine group (C-N with phenyl ring-NH) interacted with THR163 bond distance 3.09 Å as well as phenolic group (-N=O imidazole NH) interacted with TRP59 it bond distance 2.72 Å. Similarly, Cobalt complex hydrogen bonding interactions were found N=O and guanidine NH of ARG252 (bond distance 1.98 Å) as well as Nickel complex hydrogen bonding interactions were identified carbonyl oxygen of GLY249 (bond distance 2.69Å) [28 and 52]. The results suggest that the azomethine group (C-N)/phenolic group -O unit is essential to protein interactions.

Table 7
Molecular docking interaction of metal complexes with α -amylase (1HNY.pdb).

S. no	Metal complexes	Binding energy KJ/mol	No. of hydrogen bonding	Interacted amino acid residue
1	Copper complex	-296.54	2	THR163 [π -donor hydrogen bonding (3.09 Å, phenyl ring—NH of THR163)], TRP59 [conventional hydrogen bonding (2.72 Å, N=O—imidazole NH of TRP59)]
2	Cobalt complex	-291.83	1	ARG252 [conventional hydrogen bonding (1.98Å, N=O—guavinidine NH of ARG252)]
3	Nickel complex	-286.64	1	GLY249 [carbon hydrogen bonding (2.69Å, imine HC—O=C of GLY249)]

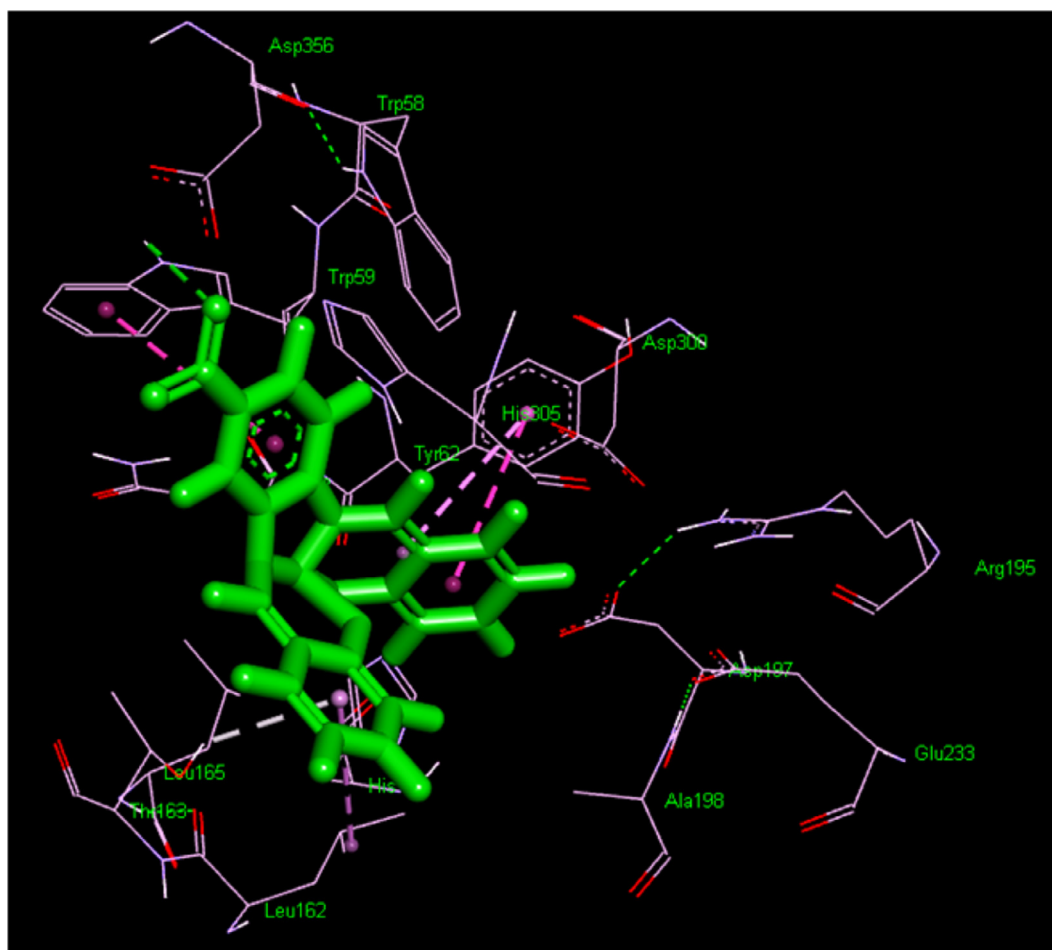


Fig. 9. Molecular docking interaction of Copper complex with α -amylase (1HNY.pdb).

4. Conclusion

The present study describes the competent synthetic pathway for the synthesis of 2,2'-((1E,1'E)-((4-nitro-1,2-phenylene) bis(azanylylidene)) bis(methanylylidene)) diphenol and Cobalt, Nickel and Copper complexes were synthesized and characterized using conductance measurements, elemental analysis, FT-IR spectra and UV-Visible spectra. The Cobalt, Nickel and Copper complexes were proven to induce the corresponding complexes by ligand coordinated to metal ions via O and N atoms. Magnetic and electronic spectral analysis shows tetrahedral geometry for the Co(II) complex, while the Ni(II) and Cu(II) complexes have square plane geometry. The powder X-ray diffraction study revealed that only Cu(II) complexes had sharp peaks, although no peaks were seen for the rest of the complexes implying their amorphous nature. The results of the geometrical parameters suggested a good conjugation effect that would aid transfer excited electron from metal ions to

ligand. The value of the energy difference between the HOMO and the LUMO suggests the title compounds stable. The electrostatic potential value has been determined as Cu(II) ($\pm 0.778e$) > Ni(II) ($\pm 0.353e$) > Co(II) ($\pm 0.214e$) complexes that support the tendency of the antioxidant activity of these complexes. The stability values of the metal complexes follow a trend: Co(II) > Ni(II) > Cu(II). Including antioxidant, antidiabetic and anti-inflammatory function of copper complex, biological activities are found to have improved action than cobalt and nickel complexes. The molecular docking studies further illustrated the intense energy interaction of metal complexes with the enzyme α -amylase.

Declaration of Competing Interest

The authors declare that they have no known competing financial interest or personal relationships that could have appeared to influence the work reported in this paper.

Acknowledgments

The theoretical calculation was reported with the aid of the TUBITAK ULAKBIM, TURKEY High Performance and Grid Computing Center (TRUBA Resources).

Supplementary materials

Supplementary material associated with this article can be found, in the online version, at doi:10.1016/j.molstruc.2021.130097.

References

- [1] S. Kundu, A.K. Pramanik, A.S. Mondal, T.K. Mondal, Ni(II) and Pd(II) complexes with new N,O donor thiophene appended Schiff base ligand: Synthesis, electrochemistry, X-ray structure and DFT calculation, *J. Mol. Struct.* 1116 (2016) 1–8.
- [2] K. Buldurun, N. Turan, A. Savci, Naki Çolak, Synthesis, Characterization, Optical Transition and Dielectric Properties of the Schiff Base Ligand and Its Cobalt(II) and Palladium(II) Complexes, *J. Saudi. Chem. Soc.* 23 (2019) 205–214.
- [3] A. Gölcü, M. Tümer, H. Demirelli, R.A. Wheatley, Cd(II) and Cu(II) complexes of polydentate Schiff base ligands: Synthesis, characterization, properties and biological activity, *Inorg. Chim. Acta.* 358 (2005) 1785.
- [4] P. Krishnamoorthy, P. Sathyadevi, K. Senthilkumar, P. Thomas Muthiah, R. Ramesh, N. Dharmaraj, Copper(II) hydrazone complexes: Synthesis, structure, DNA binding, radical scavenging and computational studies, *Inorg. Chem. Commun.* 14 (2011) 1318–1322.
- [5] M. Saha, R. Nasani, S.M. Mobin, B. Pathak, S. Mukhopadhyay, The effect of remote substitution on formation of preferential geometrical isomer of cobalt(III)-tetrazolato complexes formed via [2 + 3] cycloaddition, *Inorg. Chem. Commun.* 34 (2013) 62–67.
- [6] P. Panneerselvam, R.R. Nair, G. Vijayalakshmi, E.H. Subramanian, S.K. Sridhar, Synthesis of Schiff bases of 4-(4-aminophenyl)-morpholine as potential antimicrobial agents, *Eur. J. Med. Chem.* 40 (2005) 225–229.
- [7] M. Sankarganesh, J. Dhavethu Raja, K. Sakthikumar, R. Vijay Soloman, J. Rajesh, S. Athimoolam, V. Vijayakumar, New bio-sensitive and biologically active single crystal of pyrimidine scaffold ligand and its gold and platinum complexes: DFT, antimicrobial, 6 antioxidant, DNA interaction, molecular docking with DNA /BSA and anticancer studies, *Bioorg. Chem.* 81 (2018) 144–156.
- [8] P. Ghosh, N. Kumar, S. Kanti Mukhopadhyay, P. Banerjee, Sensitive and fluorescent Schiff base chemosensor for pico molar level fluoride detection: In vitro study and mimic of logic gate function, *Sensor Actuat B-Chem* 224 (2016) 899–906.
- [9] S.M. Saadeh, Synthesis, characterization and biological properties of Co(II), Ni(II), Cu(II) and Zn(II) complexes with an SNO functionalized ligand, *Arab. J. Chem.* 6 (2013) 191–196.
- [10] S. Vedanayaki, P. Jayaseelan, D. Sandhanamalar, R. Rajavel, Synthesis, Spectral Characterization and Antimicrobial Activities of Unsymmetrical Schiff Base Metal Complexes, *Asian J. Chem.* 23 (2011) 407–409.
- [11] R.M. Amin, N.S. Abdel-Kader, A.L. El-Ansary, Microplate assay for screening the antibacterial activity of Schiff bases derived from substituted benzopyran-4-one, *Spectrochim. Acta, Part A.* 95 (2012) 517–525.
- [12] N.M. Honsy, H.M. Mahmoud, M.H. Abdel Rhman, Spectral, optical, and cytotoxicity studies on N-(2-isonicotinoylhydrazine-carbonothioyl) benzamide and its metal complexes, *Heteroat. Chem* 29 (2018) 21415.
- [13] D. Huang, B. Ou, R.L. Prior, The chemistry behind antioxidant capacity assays, *J. Agric. Food Chem.* 53 (6) (2005) 1841–1856.
- [14] W. Al Zoubi, A. Ali Salih Al-Hamdani, S.D. Ahmed, Y. Gun Ko, A new azo-Schiff base: synthesis, characterization, biological activity and theoretical studies of its complexes, *Appl Organomet Chem* 6 (2017) 3895–3907.
- [15] S.S.A. Fathima, M.M.S. Meeran, E.R. Nagarajan, Synthesis, characterization and biological evaluation of novel 2,2'-(1,2-diphenylethane-1,2-diylidene)bis(azanylylidene)bis(pyridin-3-ol) and metal complexes: molecular docking and in silico ADMET profile, *Struct Chem* 31 (2020) 521–539 (2020).
- [16] L.I.U. Jianning, Z. Bing, W.U. Bowan, K. Zhang, H.U. Shenli, The Direct Electrochemical Synthesis of Ti(II), Fe(II), Cd(II), Sn(II), and Pb(II) Complexes with N, N-Bis(Salicylidene)-o-Phenylenediamine, *Turk. J. Chem* 31 (2007) 623–629.
- [17] Mohammed M. Ibrahim, Shaban Y. Shaban, AbdEl-Motaleb M. Ramadan, Mohammed AyadAlruqi, Gaber A.M. Mersal, Samir A. El-Shazly, Salih Al-Juaid, Ternary Copper(II) and Nickel(II) chelates of 2,2'-Bipyridyl and glycine: X-ray structures, kinetics, DNA binding and cleavage activities, *J. Mol. Struct.* 1198 (2019) 126911.
- [18] A.D.A. Becke, A new mixing of Hartree-Fock and local density-functional theories, *J. Chem. Phys.* 98 (1993) 1372–1377.
- [19] M.J. Frisch, Gaussian 09 D.01, Gaussian, Inc, Wallingford CT, 2013.
- [20] N. Islam, S. Kaya (Eds.), *Conceptual Density Functional Theory and Its Application in the Chemical Domain*, CRC Press, 2018.
- [21] T. Koopmans, Über die Zuordnung von Wellenfunktionen und Eigenwerten zu den Einzelnen Elektronen Eines Atoms, *Physica* 1 (1934) 104–113.
- [22] R.G. Parr, L.V. Szentpaly, S. Liu, Electrophilicity Index, *J. Am. Chem. Soc.* 121 (1999) 1922–1924.
- [23] F. Weinhold, C.R. Landis, E.D. Glendening, What is NBO analysis and how is it useful? *Int. Rev. in Phys. Chem.* 35 (3) (2016) 399–440.
- [24] A.E. Reed, L.A. Curtiss, F. Weinhold, Intermolecular Interactions from a Natural Bond Orbital, Donor-Acceptor Viewpoint, *Chem. Rev.* 88 (6) (1988) 899–926.
- [25] P. Prieto, M. Pineda, M. Aguilar, Spectrophotometric Quantitation of Antioxidant Capacity through the Formation of a Phosphomolybdenum Complex: Specific Application to the Determination of Vitamin E, *Anal. Biochem.* 269 (1999) 337–341.
- [26] A. Yousefi, R. Yousefi, F. Panahi, S. Sarikhani, A.R. Zolghadr, A. Bahaoddini, A. Nezhad, Novel curcumin-based pyrano [2,3-d] pyrimidine anti-oxidant inhibitors for α -amylase and α -glucosidase: Implications for their pleiotropic effects against diabetes complications, *Int. J. Biol. Macromol.* 78 (2015) 46–55.
- [27] R. Sribalan, M. Kirubavathi, G. Banupriya, V. Padmini, Synthesis and biological evaluation of new symmetric curcumin derivatives, *Bioorg. Med. Chem. Lett.* 25 (2015) 4282–4286.
- [28] G.M. Morris, M.L. Wilby, *Molecular Docking Methods*, *Mol. Biol.* 443 (2008) 365–382.
- [29] Cotton F.A., G. Wilkinson, in: *Advanced inorganic chemistry*, Wiley-Interscience, New York, 1998, pp. 1–1376.
- [30] I.P. Ejidike, P.A. Ajibade, Synthesis, Characterization, Antioxidant, and Antibacterial Studies of Some Metal(II) Complexes of Tetradentate Schiff Base Ligand: (4E)-4-[(2-(E)-[1-(2,4-Dihydroxyphenyl)ethylidene]aminoethyl)imino]pentan-2-one, *Bioinorg Chem Appl* 890734 (2015), doi:10.1155/2015/890734.
- [31] U. Singh, A.M. Malla, I.A. Bhat, A. Ahmad, M.N. Bukhari, S. Bhat, S. Anayutullah, A.A. Hashmi, Synthesis, molecular docking and evaluation of antifungal activity of Ni (II), Co (II) and Cu (II) complexes of porphyrin core macromolecular ligand, *Microb. Pathog.* 93 (2016) 172–179.
- [32] V. Sharma, E. Kundra Arora, S. Cardoza, Synthesis, antioxidant, antibacterial, and DFT study on a coumarin based salen-type Schiff base and its copper complex, *Chem. Pap* 70 (2016) 1493–1502 (2016).
- [33] M. Sivasankaran Nair, D. Arish, R. Selwin Joseyphus, Synthesis, characterization, antifungal, antibacterial and DNA cleavage studies of some heterocyclic Schiff base metal complexes, *J. Saudi. Chem. Soc.* 16 (2012) 83–88.
- [34] L.H. Abdel-Rahmana, A.M. Abu-Dief, H. Moustafab, S. Kamel Hamdan, Ni(II) and Cu(II) complexes with ONNO asymmetric tetradentate Schiff base ligand: synthesis, spectroscopic characterization, theoretical calculations, DNA interaction and antimicrobial studies, *Appl. Organometal. Chem.* 31 (2017) 3555.
- [35] P. Aravindan, C.Kamal K.Sivaraj, G.Venkatesh P.Vennila, Synthesis, Molecular structure, Spectral Characterization, Molecular docking and biological activities of (E)-N-(2-methoxy benzylidene) anthracene-2-amine and Co(II), Cu(II) and Zn(II) complexes, *J. Mol. Struct.* (2020), doi:10.1016/j.molstruc.2020.129488.
- [36] R.G. Pearson, The principle of maximum hardness, *Acc. Chem. Res.* 26 (1993) 250–255.
- [37] R.G. Pearson, Hard and Soft Acids and Bases, *J. Am. Chem. Soc.* 85 (1963) 3533–3539.
- [38] C. Morell, V. Labet, A. Grand, H. Chermette, Minimum electrophilicity principle: an analysis based upon the variation of both chemical potential and absolute hardness, *Phys. Chem. Chem. Phys.* 11 (2009) 3417–3423.
- [39] P. Fuentealba, Y. Simon-Manso, P.K. Chattaraj, Molecular Electronic Excitations and the Minimum Polarizability Principle, *J. Phys. Chem A* 104 (2000) 3185–3187.
- [40] A. Tanwar, S. Pal, D. Ranjan Roy, P. Kumar Chattaraj, Minimum magnetizability principle, *J. Chem. Phys.* 125 (2006) 056101.
- [41] R.G. Parr, R.G. Pearson, Absolute hardness: companion parameter to absolute electronegativity, *J. Am. Chem. Soc.* 105 (1983) 7512–7516.
- [42] G. Venkatesh, M. Govindaraju, C. Kamal, P. Vennila, S. Kaya, Structural, electronic and optical properties of 2,5-dichloro-p-xylylene: experimental and theoretical calculations using DFT method, *RSC Adv* 7 (2017) 1401–1412.
- [43] M. Muthukkumar, C. Kamal, G. Venkatesh, C. Kaya, S. Kaya, Israel V.M.V. Enoch, P. Vennila, R. Rajavel, Structural, spectral, DFT and biological studies on macrocyclic mononuclear ruthenium (II) complexes, *J. Mol. Struct.* 1147 (2017) 502–514.
- [44] P. Vennila, M. Govindaraju, G. Venkatesh, C. Kamal, Molecular structure, vibrational spectral assignments (FT-IR and FT-RAMAN), NMR, NBO, HOMO-LUMO and NLO properties of O-methoxybenzaldehyde based on DFT calculations, *J. Mol. Struct.* 1111 (2016) 151–156.
- [45] E.M. Zayed, F.A. El-Samahy, G.G. Mohamed, Structural, spectroscopic, molecular docking, thermal and DFT studies on metal complexes of bidentate ortho-quinone ligand, *Appl. Organometal Chem* (2019) 5065 doi.org/10.1002/aoc.5065.
- [46] S. Soudani, M. Hajji, J. Xiao Mi, C. Jelsch, F. Lefebvre, T. Guerfel, C. Ben Nasr, Synthesis, structure and theoretical simulation of a zinc(II) coordination complex with 2,3-pyridinedicarboxylate, *J. Mol. Struct.* 1199 (2020) 127015.
- [47] S. Esmailzadeh, G. Mashhadiagha, Formation constants and thermodynamic parameters of bivalent Co, Ni, Cu and Zn complexes with Schiff base ligand: experimental and DFT calculations, *Bull. Chem. Soc. Ethiop.* 31 (2017) 159–170.
- [48] R. Kavitha, S. Nirmala, R. Nithyalaji, R. Sribalan, Biological evaluation, molecular docking and DFT studies of charge transfer complexes of quinaldic acid with heterocyclic carboxylic acid, *J. Mol. Struct.* 1204 (2020) 127508.
- [49] Y. Inada, K. Mochizuki, T. Tsuchiya, H. Tsuji, Shigenobu Funahashi, Equilibrium and kinetics of the dinuclear complex formation between N,N'-ethylenebis(salicylideneiminato) copper(II) and metal(II, I) ions in acetonitrile, *Inorg. Chim. Acta.* 358 (2005) 3009–3014.
- [50] M. Sedighipour, A.H. Kianfar, W.A.K. Mahmood, M.H. Azarian, Synthesis and electronic structure of novel Schiff bases Ni/Cu (II) complexes: Evaluation of

- DNA/serum protein binding by spectroscopic studies, *Polyhedron* 129 (2017) 1–8.
- [51] R. Sribalan, G. Banupriya, V. Padmini, Synthesis, biological evaluation and *in silico* studies of tetrazole-heterocycle hybrids, *J. Mol. Struct.* 1175 (2019) 577–586.
- [52] S. Premkumar, T.N. Rekha, R.M. Asath, T. Mathavan, A.M.F. Benial, Vibrational spectroscopic, molecular docking and density functional theory studies on 2-acetylamino-5-bromo-6- methylpyridine, *Eur. J. Pharm. Sci.* 82 (2016) 115–125.